

Hexagonal Tungsten Trioxide Obtained from Peroxo-polytungstate and Reversible Lithium Electro-intercalation into Its Framework

JUNKO OI, AKIRA KISHIMOTO, AND TETSUICHI KUDO*

Institute of Industrial Science, University of Tokyo, 7-22-1, Roppongi, Minato-ku, Tokyo 106, Japan

AND MASAHIKO HIRATANI

Central Research Laboratory, Hitachi Ltd., Kokubunji, Tokyo 185, Japan

Received May 16, 1991; in revised form August 2, 1991

A hexagonal form of WO_3 ($a = 7.3244(6)$, $c = 7.6628(5)$ Å, $z = 6$) was synthesized by the low temperature sintering of an ammonium peroxo-polytungstate precursor. This compound, the N/W ratio of which is 0.015 at most, is not identical to reported hexagonal WO_3 from $\text{WO}_3 \cdot \frac{1}{3}\text{H}_2\text{O}$ because its c -axis is significantly shorter than that of the latter (7.798 Å). Powder XRD profile refinements were performed in the space group $P6_3/mcm$. We found two kinds of structural models that showed reasonably good profile agreement ($R \approx 0.07$). Both models are built up of remarkably distorted WO_6 octahedra, in which part of the O-O distances are very short (2.32 ~ 2.42 Å). Electrochemical intercalation of lithium into the present WO_3 framework was investigated using a $\text{Li}|\text{LiPF}_6|\text{WO}_3$ cell. It was found that Li was intercalated reversibly up to the composition $\text{Li}_{1.0}\text{WO}_3$. © 1992 Academic Press, Inc.

Introduction

Although hexagonal tungsten bronzes $M_x\text{WO}_3$ (M : K, Rb, etc.) have long been known, their empty framework itself (i.e., the hexagonal form of WO_3) has been synthesized only comparatively recently from a precursor $\text{WO}_3 \cdot \frac{1}{3}\text{H}_2\text{O}$ (1). More recently, it has been reported that the same compound could also be obtained by oxidation of hexagonal $(\text{NH}_4)_x\text{WO}_3$ bronze with hydrogen peroxide solution (2) or Cl_2 (3). Hexagonal WO_3 (h- WO_3) is of interest as a possible positive electrode material for batteries. In this regard, intercalation of alkaline met-

als into its framework has been investigated by some workers (2-5), though its reversibility has not been reported thoroughly.

Previously we reported (6, 7) that complex oxides, such as $(\text{K}_2\text{O})_x \cdot \text{WO}_3$ (more properly, $\text{K}_y\text{W}_{1-y/6}\text{O}_3$ with $y = 6x/(6+x)$), $(\text{Rb}_2\text{O})_x \cdot \text{WO}_3$, and $(\text{BaO})_x \cdot \text{WO}_3$ ($\text{Ba}_y\text{W}_{1-y/3}\text{O}_3$ with $y = 3x/(3+x)$), based on defective hexagonal frameworks similar to that of h- WO_3 , were obtained from peroxo-polytungstate salt of each alkaline or alkaline earth metal when they were decomposed in air at moderate temperatures. These facts led us to an attempt to synthesize h- WO_3 via ammonium peroxo-polytungstate. We succeeded in synthesis, though the compound was not fully identical to re-

* To whom correspondence should be addressed.

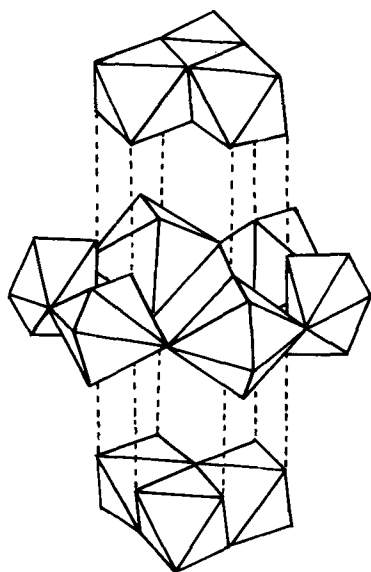


FIG. 1. Structure model of IPA (peroxo-polytungstate) anion.

ported $h\text{-WO}_3$ from $\text{WO}_3 \cdot \frac{1}{3}\text{H}_2\text{O}$. In this paper, we describe the synthesis and structure of this form of $h\text{-WO}_3$ and the reversible electrochemical Li-intercalation properties of this framework. Reported intercalation data (3–5) (e.g., potential–composition curves) are significantly diverse, probably due to structural or compositional differences of “ $h\text{-WO}_3$ ” used as a specimen.

Synthetic Procedure

Peroxo-polytungstic acid (starting material, denoted as IPA) was prepared according to the previously reported method (8). In short, metallic W powder was dissolved in 15% H_2O_2 to yield a pale yellow acidic solution. It was then dried at room temperature after excess H_2O_2 was removed catalytically with a platinized Pt net, resulting in a yellow glassy substance (IPA) with an approximate empirical formula of $2\text{WO}_3 \cdot \text{H}_2\text{O}_2 \cdot 2\text{H}_2\text{O}$. The whole structure of IPA is not thoroughly understood yet be-

cause of its noncrystalline nature. However, it was found by our recent XRD analysis (9) that the observed radial distribution function of IPA agreed very well with the calculated one from a polyanion model shown in Fig. 1, which was also consistent with IPA's IR and Raman spectra. Thus, this model is the most probable picture of the IPA polyanion to date.

Ammonium peroxo-polytungstate (a precursor, denoted by $\text{NH}_4\text{-IPA}$) was prepared as follows. A stirred mixture solution of IPA and ammonia ($\text{NH}_4/\text{W} = 2.0$, $\text{pH} = 10$) was heated at 80°C , resulting in a colorless clear solution. Neutralizing the solution by HCl yielded a white crystalline precipitate ($\text{NH}_4\text{-IPA}$), in which the molar NH_4/W ratio was about 0.8. Its IR spectrum, shown in Fig. 2, resembled that of ammonium paratungstate, $(\text{NH}_4)_{10}\text{W}_{12}\text{O}_{41} \cdot 5\text{H}_2\text{O}$, but its powder XRD pattern did not agree with this compound, nor with any reported ammonium tungstates filed in JCPDS. It is thus likely that IPA polyanions (closely related to paratungstate-B) were transformed into a peroxo version of paratungstate during the salt formation process.

When $\text{NH}_4\text{-IPA}$ was heated in air or He

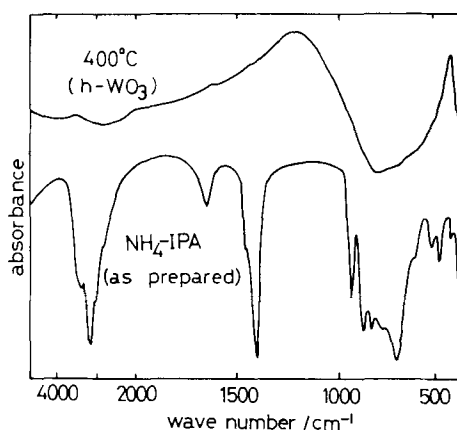


FIG. 2. IR spectra of as-prepared $\text{NH}_4\text{-IPA}$ (ammonium peroxo-polytungstate) and its derivative at 400°C ($h\text{-WO}_3$).

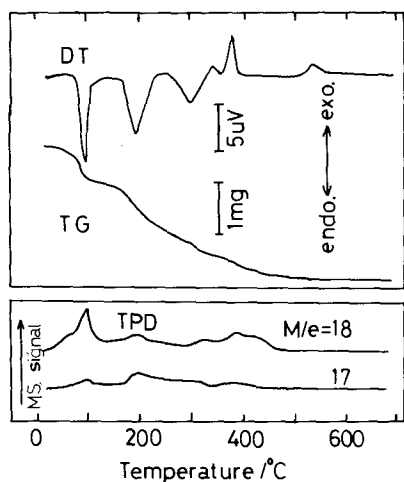


FIG. 3. TG/DT spectra of NH₄-IPA recorded in air with the sample weight of 18.6 mg and the heating rate of 10°C min⁻¹. The gas emission (TPD) spectra for $M/e = 17$ and 18 recorded in a He-stream with the same heating rate are also shown.

atmosphere, it was decomposed basically in three steps according to TG/DT spectra shown in Fig. 3. The gas emission (TPD) spectra recorded in a He-stream with a mass spectrometer (shown in the same figure) show that almost all the ammonia ($M/e = 17$) is released at temperatures up to 200°C. Figure 4 shows the powder XRD patterns recorded with NH₄-IPA heat-treated at some different temperatures. NH₄-IPA crystallizes as a hexagonal phase at about 400°C via an amorphous phase. This phase is transformed into an ordinary triclinic WO₃ near 600°C. The IR spectrum recorded with this hexagonal phase given at 400°C shows no bands due to NH₄ vibration, as shown in Fig. 2, indicating it is a hexagonal form of WO₃. The gas-chromatographically determined N/W ratio of this compound was 0.015 at most.

It is noteworthy that decomposition of ammonium paratungstate (NH₄)₁₀W₁₂O₄₁ · 5H₂O in an oxidizing atmosphere yielded no hexagonal phase, though it is known that this compound gives a hexagonal (NH₄)WO₃

bronze if it is heated in a reducing atmosphere like 10% H₂-90% He (2). In addition, h-WO₃ obtained by oxidizing this ammonium bronze with H₂O₂ has been reported to have a long c -axis (3.905 Å) which is similar to that of h-WO₃ obtained from WO₃ · $\frac{1}{3}$ H₂O.

Structural Analysis

Structural details of h-WO₃ obtained from WO₃ · $\frac{1}{3}$ H₂O have already been reported by Gerand *et al.* (1). However, h-WO₃ synthesized here is not identical to that, because their hexagonal cell parameters are obviously different: $a = 7.3244(6)$, $c = 7.6628(5)$ Å for the present h-WO₃, and $a = 7.298(2)$, $c = 7.798(3)$ Å for Gerand's.

It has been pointed out by Figlarz (4) that, in the case where h-WO₃ is synthesized by deintercalation of (NH₄) _{x} WO₃, its c -axis is remarkably shortened by the residual NH₄ cation. However, assuming that the c -axis decreases monotonically with NH₄ content, such a situation is not the case for our sample with $x \leq 0.015$, because the reported cell dimensions of (NH₄)_{0.13} · WO₃ ($a = 7.343$, $c = 7.648$ Å) (2) are very close to ours. Moreover, it should be noted that our synthetic procedure is not "deintercalation" but ther-

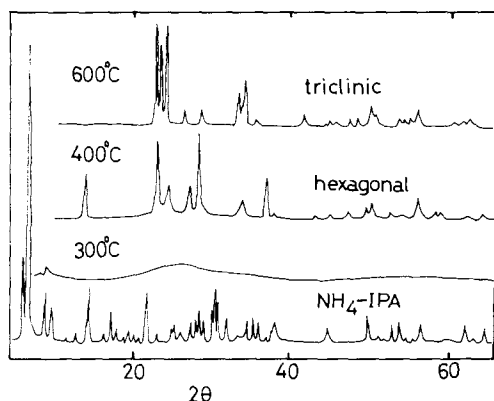


FIG. 4. Powder XRD patterns for NH₄-IPA heat-treated in air at various temperatures.

TABLE I
CRYSTALLOGRAPHIC DATA OF WO_3 AFTER
REFINEMENT (CASE 1)

Hexagonal; space group; $P6_3/mcm$ (193) $a = 7.3244(6)$ $c = 7.6628(5)$ $Z = 6$			
Atom	Atomic position Site	Occupancy	
W	$6g(x, 0, \frac{1}{2})$	$x: 0.4721(13)$	1.0
O(1)	$12j(x, y, \frac{1}{2})$	$x: 0.3745(92)$ $y: 0.183(11)$	1.0
O(2)	$12k(x, 0, z)$	$x: 0.445(19)$ $z: 0.016(27)$	0.5
Interatomic distances/Å			
W-O(1)	2×1.81	O(1)-O(2)	2×2.44
	2×2.19		2×2.67
W-O(2)	2×1.80		2×2.96
	2×2.13		2×3.08
		O(1)-O(1)	1×2.32
			1×2.42
			2×3.22

Note. $R_F = 0.068$.

mal decomposition of ammonium salt in an oxidizing or inert atmosphere.

Schlasche and Schallhorn (3) synthesized h- WO_3 having cell parameters ($a = 7.328$, $c = 7.623$ Å) very close to ours via oxidation of $(\text{NH}_4)_x\text{WO}_3$ with dry Cl_2 at 300°C , though an analytical value of the N/W ratio has not been reported (only mentioned as “ NH_4 -free”). It might be probable that our compound is identical to Schlasche’s h- WO_3 . It is interesting to note that Schlasche’s h- WO_3 and ours are formed at approximately the same temperature region. Whether they are identical or not, metastable forms of h- WO_3 seem to be plural. Thus, we attempted to perform structural determination of the present h- WO_3 .

Crystallographic data have been collected with an X-ray powder diffractometer using monochromatized $\text{CuK}\alpha$ radiation. The 2θ scanning was stepwise with the width of 0.02° and the measuring time of 5 sec. In order to diminish preferred orientation, the sample was well ground and attached softly

on a sample holder. The powder pattern could be indexed in the hexagonal system except for very weak peaks ($I/I_{200(\text{h-WO}_3)} < 0.04$) due to impurity phases at $2\theta = 26-26.5$ ($I/I_{200(\text{h-WO}_3)} < 0.04$), $29-30.5$ (< 0.02), $41-42.4$ (< 0.01), and $46.5-47$ (< 0.01). Thus, these 2θ regions were neglected in the following structural refinements, which were performed on the Rietveld method using the RIETAN computational system (10).

No obvious isolated peaks as indexed by $h0l$ ($l \neq 2n$) were found, suggesting the space groups $P6_3/mcm$, $P6_3cm$, or $P6c2$. Gerand *et al.* (1) have successfully refined their h- WO_3 in $P6_3/mcm$ with W on $6g(x, 0, \frac{1}{2})$, where x was fixed at $\frac{1}{2}$, O(1) on $12j(x, y, \frac{1}{2})$ under a restriction $x = 2y$, and O(2) on $6f(\frac{1}{2}, 0, 0)$. For our case, however, refinement using such an atomic distribution was not converged. We thus attempted to locate atoms on more general positions of $P6_3/mcm$, which had been used by Labbe *et al.* (11) for refinements of $\text{Rb}_{0.3}\text{WO}_3$ and other related hexagonal tungsten bronzes. Atomic positions after refinement, are shown in Table I together with structural parameters. The observed and calculated profiles are shown in Fig. 5 ($R_F = 0.068$).

According to the results in Table I, each WO_6 octahedron building up the present h- WO_3 is remarkably distorted. The distances between the W atom and the three adjacent oxygens are about 1.8 Å, which is a value intermediate between the single and double bonding distances, while those from other the three oxygens are much longer (2.13 and 2.19 Å), the coordination type thus being (3 + 3). Moreover, it is noted that the O-O distances between the former oxygen group are as short as 2.32-2.42 Å. These short distances are rather unfamiliar for these kinds of compounds, but not impossible because similar distances are often seen in Ta_2O_5 (12). In addition, Labbe *et al.* (11) reported that $\text{In}_{0.3}\text{WO}_3$ has a short O-O distance (2.37 Å) similar to our compounds. In

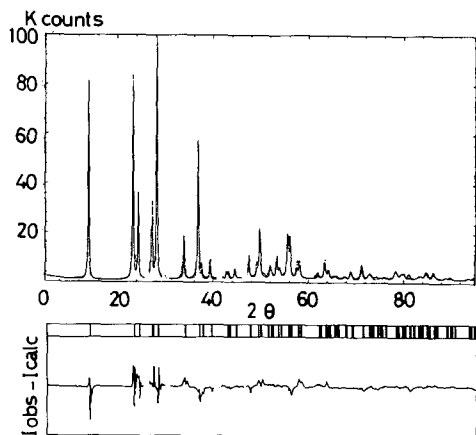


FIG. 5. The observed and calculated powder XRD profiles for hexagonal WO₃ derived from NH₄-IPA at 400°C.

contrast to this, the distortion of octahedra in the reported h-WO₃ is small, and oxygens forming hexagonal tunnels (i.e., O(1)) sit on almost their ideal sites.

We next tried to obtain a model consisting of less-distorted octahedra. Such a trial itself was unsuccessful, but we found, in this

procedure, that another *P6₃/mcm* model (Case II), in which O(1)'s were fixed at their ideal positions $12j(0.422, 0.211, 0.25)$, could be converged to the observed profile with almost the same agreement level as that in the above case. The results summarized in Table II show that similarly very short O–O distances (2.37 Å) also appear in this model. It should be mentioned that refinements in *P6₃22*, which have been used by Pye and Dickens (13) for K_{0.26}WO₃, were less successful than the above two cases and gave more distorted pictures of the WO₆ octahedron. Rather poor crystallinity of the sample (especially peak-tailing), which is often unavoidable for metastable compounds formed at relatively low temperatures, has not permitted us a definitive structural determination.

Electrochemical Results

Electrochemical intercalation of lithium into the present hexagonal WO₃,



was investigated in a 0.1 M LiPF₆/propylene carbonate solution using a gas-tight three-

TABLE II
CRYSTALLOGRAPHIC DATA OF WO₃ AFTER
REFINEMENT (CASE 2)

Hexagonal; space group; <i>P6₃/mcm</i> (193) $a = 7.3242(6)$ $c = 7.6624(5)$ $Z = 6$			
Atom	Site	Atomic position	Occupancy
W	$6g(x, 0, \frac{1}{2})$	$x: 0.4723(14)$	1.0
O(1)	$12j(x, y, \frac{1}{2})$	$x: 0.423$ $y: 0.211$	1.0
O(2)	$12k(x, 0, z)$	$x: 0.431(18)$ $z: 0.018(26)$	0.5
Interatomic distances/Å			
W–O(1)	2×1.75	O(1)–O(2)	2×2.37
	2×2.04		2×2.60
W–O(2)	2×1.80		2×2.89
	2×2.18	O(1)–O(1)	4×2.68

Note. $R_F = 0.068$.

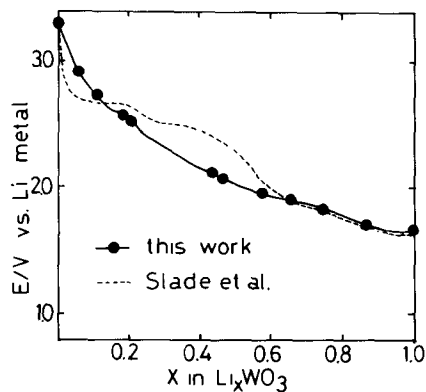


FIG. 6. Electrode potential of Li_xWO₃ (vs. Li metal) as a function of the lithium content x . The discharge curve reported by Slade *et al.* (5) for h-WO₃ derived from WO₃ · $\frac{1}{3}$ H₂O is also shown for comparison.

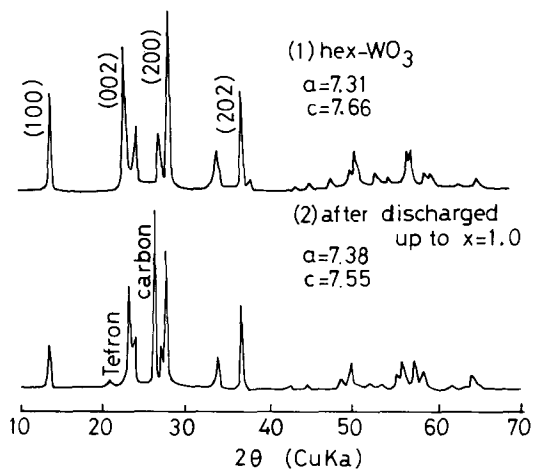


FIG. 7. Powder XRD patterns of $h\text{-WO}_3$ and $\text{Li}_{1.0}\text{WO}_3$ (after discharge). In the latter pattern, peaks due to carbon and PTFE (ingredients of the electrode) are shown.

electrode cell with counter and reference electrodes of metallic lithium. Sample electrodes were prepared as follows. A paste mixture of $h\text{-WO}_3$, artificial graphite, and poly(tetrafluoroethylene) (100:10:2 in weight) was spread on a Ni net and heated at 200°C in air for 1 hr. Experimental cells were constructed inside an Ar-filled glove box. The geometrical area of each sample electrode was $1 \times 1 \text{ cm}^2$, and its $h\text{-WO}_3$ content was about 0.05g.

First, the potential E of Li_xWO_3 was measured by means of coulometric titration. Equilibrium values of the potential after each titration are plotted in Fig. 6 as a function of the Li content x . In this figure, a voltage-composition curve of conventional $h\text{-WO}_3$ reported by Slade *et al.* (5) is also shown for comparison. Although the latter is not a strict E - x relationship in equilibrium, those two potential (or cell voltage) dependencies on the inserted Li content are quite different, especially in the range between $x = 0.3$ and 0.6 . However, both have in common a plateau or kink near $x = 0.2$, suggesting the ordering of Li at the composi-

tion near to $\text{Li}_{1/6}\text{WO}_3$, though the true mechanism of such E - x anomalies is still controversial ((14, 15) for TiS_2). It is noted that the E - x curve reported by Schlasche and Schollhorn (3) for their $h\text{-WO}_3$ also shows a kink at $x = 0.2$ - 0.3 ; however, E of this $h\text{-WO}_3$ is somewhat lower ($\sim 0.2 \text{ V}$) than ours. Except for such a kink, our E - x curve resembles that of electron-beam evaporated amorphous WO_3 (16) up to $x = 0.4$, beyond which the latter is reported to turn into a mixed phase of $\text{Li}_{0.4}\text{WO}_3$ and Li-rich WO_3 . It is noted that, according to the recent XRD study based on PDF (17), such an amorphous WO_3 film takes a cluster structure composed of fragments with a $h\text{-WO}_3$ type arrangement.

For our $h\text{-WO}_3$, contrary to evaporated films, Li-intercalation may be topotactic up to at least $x = 1.0$, because the powder profiles before and after intercalation up to this level are almost the same, as shown in Fig. 7. During intercalation, however, the a -axis is prolonged while the c -axis is shortened; the cell parameters for $\text{Li}_{1.0}\text{WO}_3$ are $a = 7.38$ and $c = 7.55 \text{ \AA}$. Topotactic insertion up to $x = 1$ indicates that Li ions are not only accommodated at cavities in the hexagonal tunnels but also at trigonal pris-

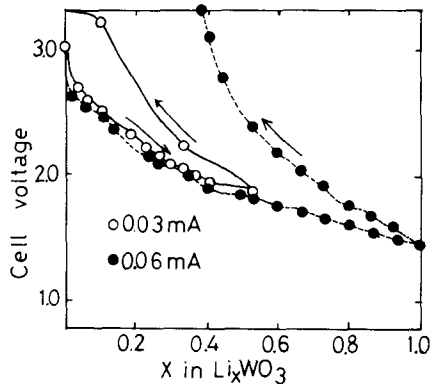


FIG. 8. Galvanostatic charge and discharge curves recorded with $h\text{-WO}_3$ in a LiPF_6 /propylene carbonate solution at room temperature.

matic 4d sites. It has been reported (3) that h-WO₃ (from WO₃ · $\frac{1}{3}$ H₂O) can accommodate Li up to $x = 1.45$ without substantial changes in the host structure.

The reversibility of Li-intercalation (re-chargeability) was tested in the ranges between $x = 0 \sim 0.5$ and $0 \sim 1.0$ under galvanostatic conditions. As shown in Fig. 8, Li can be deintercalated from Li_{0.5}WO₃ with a relatively small overvoltage, which is, however, larger than that for the intercalation process. Deintercalation from Li_{1.0}WO₃ needs a much higher overvoltage, though, considering the current is doubled in this case. It has, however, been confirmed that the electrode potential (in equilibrium) recovers about 3.0 V after prolonged charging.

Conclusion

We have synthesized a hexagonal form of WO₃ from ammonium peroxy-polytungstate. Its *c*-axis is remarkably shorter than that of reported hexagonal WO₃ from WO₃ · $\frac{1}{3}$ H₂O. Powder X-ray profile refinements gave two possible structural models, both of which were built up of significantly distorted WO₆ octahedra containing very short O–O distances. Electrochemical study revealed that intercalation of Li into the present hexagonal WO₃ framework was reversible up to the composition Li_{1.0}WO₃.

Acknowledgments

Part of this work was supported by a Grant-in-Aid for Scientific Research on Priority Areas

(402690205097) by the Ministry of Education, Science, and Culture, Japan.

References

1. B. GERAND, G. NOWOGROCKI, J. GUENOT, AND M. FIGLARZ, *J. Solid State Chem.* **29**, 429 (1979).
2. K. H. CHENG, A. J. JACOBSON, AND M. S. WHITTINGHAM, *Solid State Ionics* **5**, 355 (1981).
3. B. SCHLASCHE AND R. SCHOLLHORN, *Rev. Chim. Miner.* **19**, 534 (1982).
4. M. FIGLARZ, *Prog. Solid State Chem.* **49**, 1 (1989).
5. R. C. T. SLADE, B. C. WEST, AND G. P. HALL, *Solid State Ionics* **32/33**, 154 (1989).
6. T. KUDO, A. KISHIMOTO, AND J. OI, *Solid State Ionics* **40/41**, 567 (1990).
7. T. KUDO, J. OI, A. KISHIMOTO, AND M. HIRATANI, *Mater. Res. Bull.*, **26**, 779 (1991).
8. T. KUDO, H. OKAMOTO, K. MATSUMOTO, AND Y. SASAKI, *Inorg. Chim. Acta* **111**, L27 (1986).
9. T. NANBA, S. TAKANO, I. YASUI, AND T. KUDO, *J. Solid State Chem.* **90**(1), 47 (1991).
10. F. IZUMI, *Nippon Kessho Gakkaishi* **27**, 23 (1985).
11. P. P. LABBE, M. GOREAUD, B. RAVEAU, AND J. C. MONIER, *Acta Crystallogr. Sect. B: Struct. Crystallogr. Cryst. Chem.* **34**, 1433 (1978).
12. N. C. STEPHENSON AND R. S. ROTH, *Acta Crystallogr. Sect. B: Struct. Crystallogr. Cryst. Chem.* **27**, 1037 (1971).
13. M. F. PYE AND P. G. DICKENS, *Mater. Res. Bull.* **14**, 1397 (1979).
14. A. J. BERLINSKY, W. G. UNRUH, W. R. MCKINNON, AND R. R. HAERING, *Solid State Commun.* **31**, 135 (1979).
15. T. JACOBSEN, K. WEST, AND S. ATLUNG, *Electrochim. Acta* **27**, 1007 (1982).
16. S. K. MOHAPATRA AND S. WAGNER, *J. Electrochem. Soc.* **125**, 1603 (1978).
17. T. NANBA AND I. YASUI, *J. Solid State Chem.* **83**, 304 (1989).